Adaptive fuzzy observer and robust controller for a 2-DOF robot arm

S. Bindiganavile Nagesh*, Zs. Lendek†, A.A. Khalate‡, R. Babuška‡
*Delft University of Technology,
Mekelweg 2, 2628 CD Delft, The Netherlands (email: s.bindiganavilenagesh@student.tudelft.nl, sangeetha28@gmail.com)
†Department of Automation, Technical University of Cluj-Napoca,
Memorandumului 28, 400114 Cluj-Napoca, Romania, (email: zsofia.lendek@aut.utcluj.ro)
‡Delft Center for Systems and Control, Delft University of Technology,
Mekelweg 2, 2628 CD Delft, The Netherlands (email: {a.a.khalate, r.babuska}@tudelft.nl)

***Abstract*—Recently, adaptive fuzzy observers have been introduced that are capable of estimating uncertainties along with the states of a nonlinear system represented by an uncertain Takagi-Sugeno (TS) model. In this paper, we use such an adaptive observer to estimate the uncertainties in the state matrices of a two-degrees-of-freedom robot arm model. The TS model of the robot arm is constructed using the sector nonlinearity approach. The estimates are used in updating the model, and the updated model is used to design a controller for the robot arm. We analyze the improvement in the achievable controller performance when using the adaptive observer.**

I. Introduction

A large class of nonlinear systems can be represented by Takagi-Sugeno (TS) fuzzy models [1], [5]. The TS model consists of a rule base, where the consequent of each rule is a linear or affine state-space model. One way to obtain an exact TS representation of a given nonlinear model is the sector nonlinearity approach [4].

Uncertainty that exists in the parameters of the nonlinear system can be represented in an uncertain TS fuzzy model as unmodelled dynamics. Adaptive observers that are able to estimate the unmodelled dynamics have been developed in [2]. These observers are designed such that, given an upper bound on the uncertainty norm, the error dynamics are asymptotically stable and the uncertainties are estimated. The observer design is based on a common quadratic Lyapunov function.

In this paper, we consider a 2-DOF robot arm operating in the horizontal plane. A TS model of the robot arm is constructed using the sector nonlinearity approach. The uncertainty in the damping coefficients in the individual joints is represented as uncertainty in the state matrices and we use an adaptive observer to estimate this uncertainty. All the states are measured and hence the adaptive observer estimates only the uncertainties. The design of uncertainty estimation experiments based on the structure of the TS fuzzy model is also investigated.

We analyze the influence of the obtained uncertainty estimates on the controller design. The estimates given by the adaptive observer are used to update the TS model of the robot arm. Subsequently, the updated model is used to re-design a stabilizing controller. We analyze the improvements in the controller performance due to the use of an updated model. To use the updated model in controller design, we need a design method which uses the same uncertainty distribution structure as the adaptive observer. Hence, we use a robust controller design approach for the same uncertainty distribution structure. Uncertainty estimation in the presence of a stabilizing controller is also studied.

The paper is organized as follows. Section II presents the robot arm model. In Section III, an adaptive observer is designed for the robot arm. In this section we also discuss the use of the structure of the TS model in setting up the uncertainty estimation experiments. Section IV presents the robust controller design for the robot arm. Section V presents the uncertainty estimation in the presence of a controller stabilizing the plant. Finally, Section VI concludes the paper.

II. TS model of the 2-DOF robot arm

Robot manipulators are of great importance for automation not only in traditional industries, such as car manufacturing, but more importantly in new upcoming domains, such as agricultural harvesting and product handling, or in household tasks. Rather than big, heavy and therefore dangerous, these new-generation robots need to be human-friendly. This requires light-weight, soft and compliant mechanical design, combined with novel control solutions to achieve the desired precision and repeatability.

In this paper we use an adaptive observer to estimate the uncertainties in the state matrices of a 2-DOF robot arm model. The TS model of the robot arm is constructed using the sector nonlinearity approach. The estimates are used in updating the arm model, and the updated model is used to design a controller for the arm.

A schematic representation of a 2-DOF robot arm is given in Figure 1.

The nonlinear model of the arm operating in the horizontal plane is:

$$M_R(\theta)\ddot{\theta} + C_R\dot{\theta} = \tau \tag{1}$$

with

$$M_R(\theta) = \begin{bmatrix} P_1 + P_2 + 2P_3\cos\theta_2 & P_2 + P_3\cos\theta_2 \\ P_2 + P_3\cos\theta_2 & P_2 \end{bmatrix} \tag{2}$$

$$C_R(\theta,\dot{\theta}) = \begin{bmatrix} b_1 - P_3\dot{\theta}_2\sin\theta_2 & -P_3(\dot{\theta}_1+\dot{\theta}_2)\sin\theta_2 \\ -P_3\dot{\theta}_2\sin\theta_2 & b_2 \end{bmatrix} \tag{3}$$

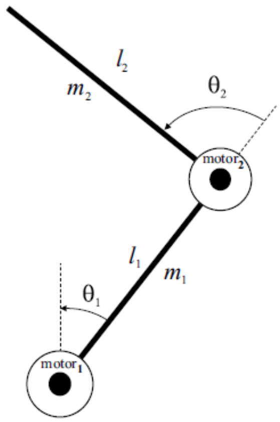

Fig. 1. A 2-DOF robot arm.

where M_R is the mass matrix, C_R is the Coriolis and centrifugal force matrix, θ_1 and θ_2 are the joint angles, $\dot{\theta}_1$ and $\dot{\theta}_2$ are the angular velocities, τ_1 and τ_2 are the torque inputs, $P_1 = m_1 {c_1}^2 + m_2 {l_1}^2 + I_1$, $P_2 = m_2 {c_2}^2 + I_2$, $P_3 = m_2 l_1 c_2$, l_1 and l_2 are the lengths, m_1 and m_2 are the masses, I_1 and I_2 are the inertias, c_1 and c_2 are the centers of mass of the first and the second link, respectively, and b_1 and b_2 are the damping coefficients of the first and second joint, respectively.

The above model can be written in the state-space form as follows:

$$\dot{\boldsymbol{x}} = \begin{bmatrix} -M_R^{-1} C_R & 0 \\ I & 0 \end{bmatrix} \boldsymbol{x} + \begin{bmatrix} M_R^{-1} \\ 0 \end{bmatrix} \tau \tag{4}$$

where $\boldsymbol{x} = [\dot{\theta}_1 \quad \dot{\theta}_2 \quad \theta_1 \quad \theta_2]^T$, or as

$$\dot{\boldsymbol{x}} = A(\theta, \dot{\theta}) \boldsymbol{x} + B(\theta) \tau \tag{5}$$

where

$$A = \begin{bmatrix} A_{11} & A_{12} & 0 & 0 \\ A_{21} & A_{22} & 0 & 0 \\ 1 & 0 & 0 & 0 \\ 0 & 1 & 0 & 0 \end{bmatrix}$$

$$\begin{aligned} A_{11} &= \frac{P_2(b_1 - P_3 \dot{\theta}_2 \sin(\theta_2)}{P_3^2 \cos^2(\theta_2) - P_1 P_2} - \frac{P_3 \dot{\theta}_2 \sin(\theta_2)(P_2 + P_3 \cos(\theta_2))}{P_3^2 \cos^2(\theta_2) - P_1 P_2} \\ A_{12} &= -\frac{b2(P_2 + P_3 \cos(\theta_2))}{P_3^2 \cos^2(\theta_2) - P_1 P_2} - \frac{P_2 P_3 \sin(\theta_2)(\dot{\theta}_1 + \dot{\theta}_2)}{P_3^2 \cos^2(\theta_2) - P_1 P_2} \\ A_{21} &= \frac{P_3 \dot{\theta}_2 \sin(\theta_2)(P_1 + P_2 + 2P_3 \cos(\theta_2))}{P_3^2 \cos^2(\theta_2) - P_1 P_2} \\ &\quad - \frac{(P_2 + P_3 \cos(\theta_2))(b_1 - P_3 \dot{\theta}_2 \sin(\theta_2))}{P_3^2 \cos^2(\theta_2) - P_1 P_2} \\ A_{22} &= \frac{b_2(P_1 + P_2 + 2P_3 \cos(\theta_2))}{P_3^2 \cos^2(\theta_2) - P_1 P_2} \\ &\quad + \frac{P_3 \sin(\theta_2)(P_2 + P_3 \cos(\theta_2))(\dot{\theta}_1 + \dot{\theta}_2)}{P_3^2 \cos^2(\theta_2) - P_1 P_2} \end{aligned} \tag{6}$$

$$B = \begin{bmatrix} -\frac{P_2}{P_3^2 \cos^2(\theta_2) - P_1 P_2} & \frac{P_2 + P_3 \cos(\theta_2)}{P_3^2 \cos^2(\theta_2) - P_1 P_2} \\ \frac{P_2 + P_3 \cos(\theta_2)}{P_3^2 \cos^2(\theta_2) - P_1 P_2} & -\frac{P_1 + P_2 + 2P_3 \cos(\theta_2)}{P_3^2 \cos^2(\theta_2) - P_1 P_2} \end{bmatrix}$$

Examining the above nonlinear model reveals the presence of six nonlinear terms:

$$\begin{aligned} z_1 &= \frac{1}{{\mathrm{P}_3}^2 \cos(\theta_2)^2 - \mathrm{P}_1 \mathrm{P}_2} & z_2 &= \frac{\cos(\theta_2)}{{\mathrm{P}_3}^2 \cos(\theta_2)^2 - \mathrm{P}_1 \mathrm{P}_2} \\ z_3 &= \frac{\dot{\theta}_2 \sin(\theta_2)}{{\mathrm{P}_3}^2 \cos(\theta_2)^2 - \mathrm{P}_1 \mathrm{P}_2} & z_4 &= \frac{\dot{\theta}_2 \cos(\theta_2) \sin(\theta_2)}{{\mathrm{P}_3}^2 \cos(\theta_2)^2 - \mathrm{P}_1 \mathrm{P}_2} \\ z_5 &= \frac{\dot{\theta}_1 \sin(\theta_2)}{{\mathrm{P}_3}^2 \cos(\theta_2)^2 - \mathrm{P}_1 \mathrm{P}_2} & z_6 &= \frac{\dot{\theta}_1 \cos(\theta_2) \sin(\theta_2)}{{\mathrm{P}_3}^2 \cos(\theta_2)^2 - \mathrm{P}_1 \mathrm{P}_2} \end{aligned}$$

The term A_{11} for instance can be written in terms of the above nonlinearities as

$$A_{11} = P_2 b_1 z_1 - 2P_3 P_2 z_3 - P_3^2 z_4$$

Similarly all other elements in A and B can be written in terms of the above six nonlinearities. Using the sector nonlinearity approach [4], TS models of the form

$$R_i : \text{If } z_1 \text{ is } N_i^1 \text{ and } z_2 \text{ is } N_i^2, \dots \text{ and } z_p \text{ is } N_i^p, \text{ then}$$
$$\begin{aligned} \dot{\boldsymbol{x}} &= A_i \boldsymbol{x} + B_i \boldsymbol{u} \\ \boldsymbol{y} &= C_i \boldsymbol{x} \end{aligned}$$

for $i = 1, 2, \dots, r$ can be constructed. The TS model can be written as:

$$\begin{aligned} \dot{\boldsymbol{x}} &= \sum_{i=1}^{r} h_i(\boldsymbol{z})(A_i \boldsymbol{x} + B_i \boldsymbol{u}) \\ \boldsymbol{y} &= \sum_{i=1}^{r} h_i(\boldsymbol{z})(C_i \boldsymbol{x}) \end{aligned} \tag{7}$$

where r is the number of rules, $\boldsymbol{x}$ is the state vector, $\boldsymbol{u}$ is the input vector, $\boldsymbol{y}$ is the output vector, $\boldsymbol{x} \in \mathbb{R}^{n_x}$, $\boldsymbol{u} \in \mathbb{R}^{n_u}$, and $\boldsymbol{y} \in \mathbb{R}^{n_y}$, $\boldsymbol{z} = [z_1, z_2 \dots z_p]^T$ is the vector of scheduling variables, $A_i \in \mathbb{R}^{n_x \times n_x}$, $B_i \in \mathbb{R}^{n_x \times n_u}$, $i = 1, 2, \dots, r$ are known state and input matrices of the individual linear models that are combined to represent the nonlinear system, and $h_i(\boldsymbol{z})$ are normalized membership degrees of the rules. Since we have six nonlinear terms, $p = 6$, and the number of rules is $r = 2^6$.

However, if we neglect the Coriolis and centrifugal forces in C_R, i.e., assuming that $\dot{\theta}_1 \sin(\theta_2) \simeq 0$ and $\dot{\theta}_2 \sin(\theta_2) \simeq 0$, leading to $C_R = \begin{bmatrix} b_1 & 0 \\ 0 & b_2 \end{bmatrix}$, we have only the two following nonlinearities:

$$z_1 = \frac{1}{P_3^2 \cos(\theta_2)^2 - P_1 P_2} \tag{8}$$

and

$$z_2 = \frac{\cos(\theta_2)}{{P_3}^2 \cos(\theta_2)^2 - P_1 P_2} \tag{9}$$

and we obtain the state-space model

$$\dot{\boldsymbol{x}} = A(z_1, z_2) \boldsymbol{x} + B(z_1, z_2) \boldsymbol{u} \tag{10}$$

where $\boldsymbol{u}$ is the input voltage $[u_1\, u_2]^T$ and the actual input torque τ is represented in terms of the input voltage,

$$\tau = \begin{bmatrix} k_{m1} & 0 \\ 0 & k_{m2} \end{bmatrix} \begin{bmatrix} u_1 \\ u_2 \end{bmatrix} \tag{11}$$

$$A = \begin{bmatrix} P_2 b_1 z_1 & -P_2 b_2 z_1 - P_3 b_2 z_2 & 0 & 0 \\ -P_2 b_1 z_1 - P_3 b_1 z_2 & b_2 z_1 (P_1 + P_2) + 2 P_3 b_2 z_2 & 0 & 0 \\ 1 & 0 & 0 & 0 \\ 0 & 1 & 0 & 0 \end{bmatrix} \tag{12}$$

and

$$B = \begin{bmatrix} -P_2 k_{m1} z_1 & k_{m2}(P_2 z_1 + P_3 z_2) \\ k_{m1}(P_2 z_1 + P_3 z_2) & -k_{m2}(2 P_3 z_2 + z_1(P_1 + P_2)) \\ 0 & 0 \\ 0 & 0 \end{bmatrix} \tag{13}$$

where k_{m1} and k_{m2} are voltage-to-torque motor gains.

To obtain the values of the parameters, we first identified the parameters of the DC motors in the individual joints, using SISO identification experiments on a small-scale robot arm, with the bandwidth of operation around 5 Hz. These values were used afterwards to find the values of P_1, P_2 and P_3 through nonlinear optimization based on input-output data from MIMO experiments on the robot arm. The values obtained through the nonlinear optimization are $k_{m1} = 6.59$, $k_{m2} = 1.51$, $b_1 = 1.22$, $b_2 = 0.24$, $P_1 = 0.0191$, $P_2 = 0.00039$ and $P_3 = 0.00000967$. The angles are limited to $-1.6 \leq \theta_1 \leq 1.6$ rad and $-1.7 \leq \theta_2 \leq 1.64$ rad.

We have compared the model outputs for the model with a complete C_R (Coriolis) matrix and with a simplified C_R matrix consisting of only damping coefficients. The comparison between the angular positions of the two links of the robot arm model when excited by a multisine input is presented in Figures 2 and 3.

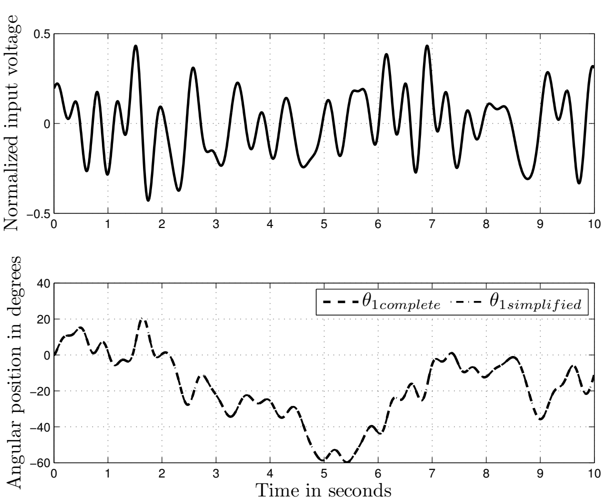

Fig. 2. Comparison between the model outputs – link 1.

It can be observed that the outputs are almost the same. This indicates that in the considered setting we can neglect the Coriolis and centrifugal forces in the nonlinear model and in the sequel we use the simplified nonlinear model. With the model parameters as described above, a 4-rule TS model is

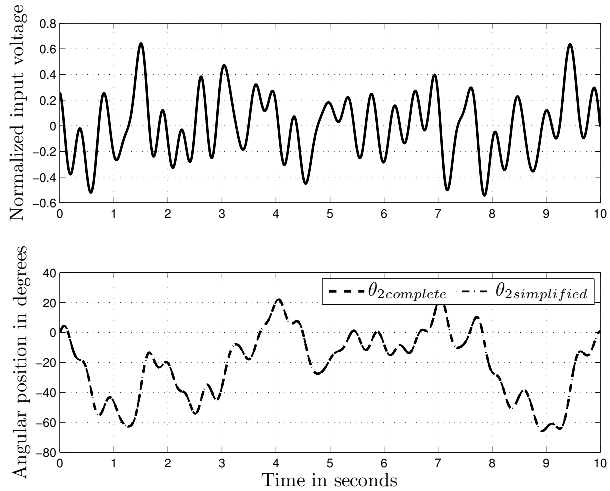

Fig. 3. Comparison between the model outputs – link 2.

constructed by using the sector nonlinearity approach [4]. The rules of the TS model are of the form

R_i : If z_1 is N_i^1 and z_2 is N_i^2 then

$$\dot{\boldsymbol{x}} = A_i \boldsymbol{x} + B_i \boldsymbol{u} \qquad \text{for } i = 1, 2, 3, 4 \tag{14}$$

and membership functions obtained are

$$\begin{aligned} w_{11}(z_1) &= \frac{z_{1max} - z_1}{z_{1max} - z_{1min}} \\ w_{12}(z_1) &= \frac{z_1 - z_{1min}}{z_{1max} - z_{1min}} \\ w_{21}(z_2) &= \frac{z_{2max} - z_2}{z_{2max} - z_{2min}} \\ w_{22}(z_2) &= \frac{z_2 - z_{2min}}{z_{2max} - z_{2min}} \end{aligned} \tag{15}$$

Since all the states are measured, the above model can be rewritten as

$$\begin{aligned} \dot{\boldsymbol{x}} &= \sum_{i=1}^{r} h_i(\boldsymbol{z})(A_i \boldsymbol{x} + B_i \boldsymbol{u}) \\ \boldsymbol{y} &= C \boldsymbol{x} \end{aligned}$$

with $C = I$, and the normalized membership values of each rule are given by $h_i(z) = \dfrac{w_i(z)}{\sum_{i=1}^{r} w_i(z)}$ and $w_1(\boldsymbol{z}) = w_{11}(z_1) w_{21}(z_2)$, $w_2(\boldsymbol{z}) = w_{11}(z_1) w_{22}(z_2)$, $w_3(\boldsymbol{z}) = w_{12}(z_1) w_{21}(z_2)$, and $w_4(\boldsymbol{z}) = w_{12}(z_1) w_{22}(z_2)$. The matrices A_i and B_i, $i = 1, 2, 3, 4$ are obtained by substituting the minimum and maximum values of the uncertainties, respectively. For instance, the matrices of the first local model are

$$A_1 = \begin{bmatrix} -63.77 & 12.89 & 0 & 0 \\ 65.35 & -629.24 & 0 & 0 \\ 1 & 0 & 0 & 0 \\ 0 & 1 & 0 & 0 \end{bmatrix} \tag{16}$$

$$B_1 = \begin{bmatrix} 344.93 & -81.16 \\ -353.48 & 3961.4 \\ 0 & 0 \\ 0 & 0 \end{bmatrix} \quad (17)$$

Matrices A_i and B_i for $i = 2, 3, 4$ can computed in the same way. The output matrix is the identity matrix for all the four rules, i.e., all the states are available as outputs.

III. Adaptive observer design

An adaptive observer that can estimate uncertainties in the state matrices of a TS model has been proposed in [3]. We use this observer to estimate the uncertainties, and later on, to improve the performance of the controller designed for the robot arm.

Since the states are measured and the uncertainties are present only in the state matrices, the uncertain TS model is of the form

$$\begin{aligned} \dot{\boldsymbol{x}} &= \sum_{i=1}^{r} h_i(\boldsymbol{z})(A_i\boldsymbol{x} + B_i\boldsymbol{u} + M_i A_{\delta i}\boldsymbol{x}) \\ \boldsymbol{y} &= C\boldsymbol{x} \end{aligned}$$

where $C = I$ and the product $M_i A_{\delta i}$ represents the uncertainty in the state matrices. We assume that this uncertainty is due to the damping coefficients.

The adaptive observer that is used to estimate the uncertainties is of the form

$$\begin{aligned} \dot{\widehat{\boldsymbol{x}}} &= \sum_{i=1}^{r} h_i(\boldsymbol{z})(A_i\boldsymbol{x} + B_i\boldsymbol{u} + L_i(\boldsymbol{y} - \widehat{\boldsymbol{y}}) + M_i(\widehat{A}_{\delta i}\widehat{\boldsymbol{x}})) \\ \widehat{\boldsymbol{y}} &= C\widehat{\boldsymbol{x}} \end{aligned}$$

together with the update law

$$\dot{\widehat{A}}_{\delta i} = h_i(\boldsymbol{z}) M_i^T P C^{\dagger} \boldsymbol{e}_y \widehat{x}^T \qquad i = 1, 2, \ldots, r \quad (18)$$

where L_i, $i = 1, 2, \ldots, r$ are the observer gain matrices for each rule, P is the Lyapunov matrix, and $C^{\dagger}$ is the Moore-Penrose pseudoinverse of the output matrix C. Given that the uncertainty norm satisfies $\|A_{\delta i}\| \leq \mu_{max}$, the update laws are determined so that the estimation errors $(\boldsymbol{x} - \widehat{\boldsymbol{x}})$ and $(A_{\delta i} - \widehat{A}_{\delta i})$ asymptotically converge to zero.

Considering the uncertainty in the values of damping coefficients b_1 and b_2 to be 0.05 and 0.0002 respectively, we have

$$A_{\delta i} = \begin{bmatrix} -0.26 & 0.01 & 0 & 0 \\ 0.26 & -0.52 & 0 & 0 \end{bmatrix} \quad (19)$$

for $i = 1, 2, 3, 4$. The uncertainty distribution matrices are

$$M_i = \begin{bmatrix} 1 & 0 \\ 0 & 1 \\ 0 & 0 \\ 0 & 0 \end{bmatrix} \quad (20)$$

for $i = 1, 2, 3, 4$. The product $M_i A_{\delta i}$ is referred to as the uncertainty distribution structure, with the notation $\Delta A_i = M_i A_{\delta i}$.

A multi-sine input signal limited in frequency to 3 Hz that activates all rules is used to excite the system. This input is chosen such that the states do not reach their saturation limits. The duration of 50 s for the simulation of the adaptive observer has been experimentally determined as sufficient to obtain a significant reduction in the uncertainty estimation error.

With the maximum uncertainty norm $\|A_{\delta i}\|$ being 0.6040, we can design an adaptive observer with $\mu_{max} = 2$. However, repeating the experiments for different values of μ_{max}, we observed that as the value of μ_{max} for which the adaptive observer is designed increases, the uncertainty estimation error given by $\sum_{i=1}^{r} trace(\bar{A}_{\delta i}^T \bar{A}_{\delta i})$ decreases at a faster rate. Therefore, we have redesigned the observer for $\mu_{max} = 200$. For this value, we obtain

$$P = \begin{bmatrix} 557.85 & 0.01 & 0.00 & 0.00 \\ 0.01 & 557.69 & 0.00 & 0.00 \\ 0.00 & 0.00 & 557.90 & 0.00 \\ 0.00 & 0.00 & 0.00 & 557.90 \end{bmatrix}$$

and the observer gains L_i, $i = 1, 2, \ldots, r$ are

$$L_1 = \begin{bmatrix} 2681.5 & 39.06 & 0.49 & 0 \\ 39.06 & 2116.5 & 0 & 0.50 \\ 0.49 & 0 & 2745.1 & 0 \\ 0 & 0.50 & 0 & 2745.1 \end{bmatrix}$$

$$L_2 = \begin{bmatrix} 2681.5 & 37.99 & 0.49 & 0 \\ 37.99 & 2117.2 & 0 & 0.50 \\ 0.49 & 0 & 2745.1 & 0 \\ 0 & 0.50 & 0 & 2745.1 \end{bmatrix}$$

$$L_3 = \begin{bmatrix} 2681.5 & 39.06 & 0.49 & 0 \\ 39.06 & 2116.5 & 0 & 0.50 \\ 0.49 & 0 & 2745.1 & 0 \\ 0 & 0.50 & 0 & 2745.1 \end{bmatrix}$$

$$L_4 = \begin{bmatrix} 2681.5 & 37.99 & 0.49 & 0 \\ 37.99 & 2117.2 & 0 & 0.50 \\ 0.49 & 0 & 2745.1 & 0 \\ 0 & 0.50 & 0 & 2745.1 \end{bmatrix}$$

After executing the adaptive observer for 50 s, the uncertainty estimates are:

$$\begin{aligned} \widehat{A}_{\delta 1} &= \begin{bmatrix} -0.30 & 0.01 & 0 & 0 \\ 0.31 & -0.55 & 0 & -0.01 \end{bmatrix} \\ \widehat{A}_{\delta 2} &= \begin{bmatrix} -0.06 & 0 & 0 & 0 \\ 0.04 & -0.18 & 0 & 0 \end{bmatrix} \\ \widehat{A}_{\delta 3} &= \begin{bmatrix} -0.19 & 0 & 0 & 0 \\ 0.15 & -0.52 & 0 & 0 \end{bmatrix} \\ \widehat{A}_{\delta 4} &= \begin{bmatrix} -0.09 & 0 & 0 & 0 \\ 0.08 & -0.20 & 0 & 0 \end{bmatrix} \end{aligned}$$

The activation of the rules is shown in Figure 4. The uncertainty estimation error corresponding to each rule is given in Figure 5 for $\mu_{max} = 2$, $\mu_{max} = 20$ and $\mu_{max} = 200$. Note that the uncertainty estimation error converges faster for larger values of μ_{max}.

The estimation error also converges faster for the rules with higher activation degrees. For instance, the activation degrees of R_1 and R_3 are higher than those of R_2 and R_4 and the uncertainty estimation error is smaller in case of R_1

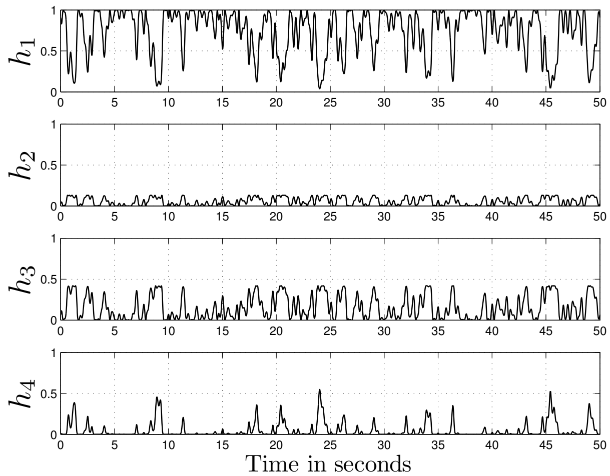

Fig. 4. Activation of the rules.

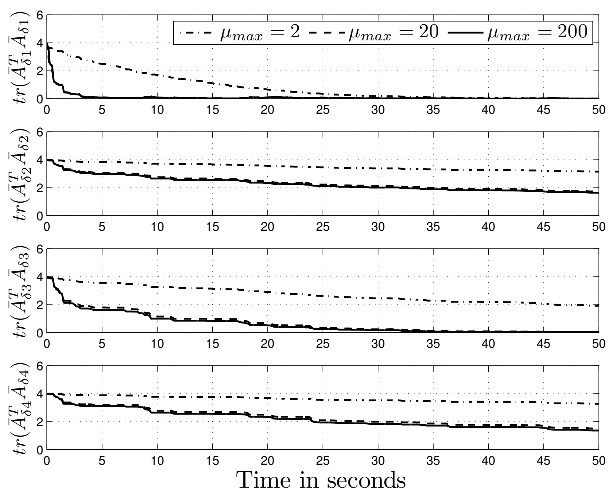

Fig. 5. Uncertainty estimation error with different values of μ_{max}.

and R_3 compared to R_2 and R_4. This is due to the update laws of the uncertainty matrices, which depend on the degree of rule activation.

The nonlinearities in the TS model depend only on θ_2. Moreover, if the uncertainty is only in b_2, then the uncertainties can be estimated using only u_2, thus avoiding the need to design the input u_1. Let us consider this case, i.e., the uncertainty only in b_2. Then, assuming that the true uncertainties are

$$A_{\delta i} = \begin{bmatrix} 0 & 0.01 & 0 & 0 \\ 0 & -0.52 & 0 & 0 \end{bmatrix}$$

the estimates of the uncertainties using input u_2 alone with $\mu_{max} = 200$ are obtained as

$$\begin{aligned} \widehat{A}_{\delta 1} &= \begin{bmatrix} 0.02 & 0.01 & 0 & 0 \\ -0.02 & -0.54 & 0 & -0.02 \end{bmatrix} \\ \widehat{A}_{\delta 2} &= \begin{bmatrix} 0 & 0 & 0 & 0 \\ 0 & -0.18 & 0 & 0 \end{bmatrix} \\ \widehat{A}_{\delta 3} &= \begin{bmatrix} 0 & 0.01 & 0 & 0 \\ 0 & -0.54 & 0 & 0 \end{bmatrix} \\ \widehat{A}_{\delta 4} &= \begin{bmatrix} 0 & 0 & 0 & 0 \\ 0 & -0.21 & 0 & 0 \end{bmatrix} \end{aligned}$$

For rules 1 and 3, the uncertainty estimates are close to the true values. Better estimates for rules 2 and 4 can be obtained if the simulation is run longer. Thus, we can exploit the uncertainty structure in the TS model to design the estimation experiments.

IV. Robust controller design

The estimates obtained in the previous section are now used to update the model of the robot arm. To analyze the achievable improvements in the controller performance, we design a controller with the same uncertainty distribution structure as in the adaptive observer, i.e., $\Delta A_i = M_i A_{\delta i}$. Robust control designs similar to those available in [6] can be derived for the uncertainty distribution structure $M_i A_{\delta i}$. Using a common quadratic Lyapunov function $V(\boldsymbol{x}) = \boldsymbol{x}^T P \boldsymbol{x}$, the following theorems present the robust controller design with an associated decay rate of α and the maximum uncertainty norms for which the controller can guarantee stability. The controller is a parallel distributed compensator with each rule of the controller containing a linear feedback law for each corresponding rule of the TS model.

Consider the TS fuzzy system,

$$\dot{\boldsymbol{x}} = \sum_{i=1}^{r} h_i(\boldsymbol{z})(A_i \boldsymbol{x} + B_i \boldsymbol{u} + M_i A_{\delta i} \boldsymbol{x}) \tag{21}$$

and the control law

$$\boldsymbol{u} = -\sum_{i=1}^{r} h_i(\boldsymbol{z}) F_i \boldsymbol{x} \tag{22}$$

where h_i are the normalized membership functions.

Theorem 1: The uncertain fuzzy system (21) *is stabilized by the controller* (22) *and the closed-loop system has a decay rate of at least* α *if there exist a common positive definite matrix* P $(X = P^{-1})$ *and* N_i, $i = 1, 2, \ldots, r$ $(N_i = F_i X)$ *that satisfy*

$$\underset{\mu_i{}^2, X, N_1, N_2 \ldots N_r}{\textit{maximize}} \quad \sum_{i=1}^{r} \beta_i {\mu_i}^2$$

subject to

$$\begin{aligned} & X > 0, \\ & \widehat{S}_{ii} < 0, \\ & \widehat{T}_{ij} < 0, \qquad i, j = 1, 2, \ldots, r \text{ and } i < j \text{ s.t } h_i\, h_j \neq 0 \end{aligned}$$

where r is the number of rules, F_i are the controller gains, α is the specified decay rate, $\beta_i, i = 1, 2, \ldots, r$ are design parameters and $\widehat{S}_{ii}$ and $\widehat{T}_{ij}, i, j = 1, 2, \ldots, r$ are given by

$$\widehat{S}_{ii} = \begin{bmatrix} \left(\widehat{S}_{ii}^{11} + 2\alpha X\right) & M_i & X \\ M_i^T & -I & 0 \\ X & 0 & -\frac{1}{\mu_i^2} I \end{bmatrix} \tag{23}$$

$$\widehat{T}_{ij} = \begin{bmatrix} \left(\widehat{T}_{ij}^{11} + 4\alpha X\right) & M_i & M_j & X & X \\ M_i^T & -I & 0 & 0 & 0 \\ M_j^T & 0 & -I & 0 & 0 \\ X & 0 & 0 & -\frac{1}{\mu_i^2} I & 0 \\ X & 0 & 0 & 0 & -\frac{1}{\mu_j^2} I \end{bmatrix} \tag{24}$$

with $\widehat{S}_{ii}^{11} = A_i X + X A_i^T - B_i N_i - N_i^T B_i^T$, *and* $\widehat{T}_{ij}^{11} = A_i X + X A_i^T + A_j X + X A_j^T - B_i N_j - N_j^T B_i^T - B_j N_i - N_i^T B_j^T$.

The maximum uncertainty bounds μ_i on $A_{\delta i}$ ($\|A_{\delta i}\| \leq \mu_i$) for which the controller guarantees stability is obtained as part of the control design procedure. Constraints on the control input can also be specified, as follows.

Theorem 2: [6] The system (21) *is stabilized by* (22) *and given an upper bound ϕ on the initial state (i.e., $\|\boldsymbol{x}(0)\| \leq \phi$), the constraint on the control input $\|\boldsymbol{u}(t)\| \leq \zeta$ is satisfied for all $t > 0$, if the following LMIs are satisfied*

$$\begin{bmatrix} X & N_i^T \\ N_i & \zeta^2 I \end{bmatrix} \geq 0 \quad \textit{for } i = 1, 2, \ldots, r$$
$$X \geq \phi^2 I$$

Using Theorems 1 and 2, a robust controller is designed for the nominal TS model with $\alpha = 1$, $\phi = 1$ and $\zeta = 1$. The maximum uncertainty norms obtained from the controller design are $\mu_i = 0.63$, $i = 1, 2, 3, 4$. These values guarantee stability of the nominal model since the maximum uncertainty norm of the four rules is 0.6040. When the adaptive observer is used to estimate the uncertainties, the norms of the residual uncertainty, i.e., $\|A_{\delta i} - \widehat{A}_{\delta i}\|$ after 50 s are obtained as 0.0738, 0.4195, 0.1360 and 0.3774 for the four rules. Consequently, the norm of the uncertainties for which a controller will have to be designed with the updated model, are smaller, and an improvement in the controller performance can be expected. Designing the controller with $\alpha = 2$, $\phi = 1$ and $\zeta = 1$ for the updated model, the maximum uncertainty norms guaranteed to be stabilized by the controller are $\mu_i = 0.47$, $i = 1, 2, 3, 4$.

V. Closed-loop uncertainty estimation in a controlled system

In the case of systems for which open-loop experiments cannot be performed (such as open-loop unstable systems), closed-loop uncertainty estimation must be considered. In this section, we investigate this case. A robust controller that stabilizes the system is designed for the nominal TS model with $\alpha = 1$, $\phi = 1$ and $\zeta = 1$, and an adaptive observer with $\mu_{max} = 200$ is designed to estimate the uncertainties. The activation of the different rules and the individual uncertainty estimation errors are shown in Figures 6 and 7.

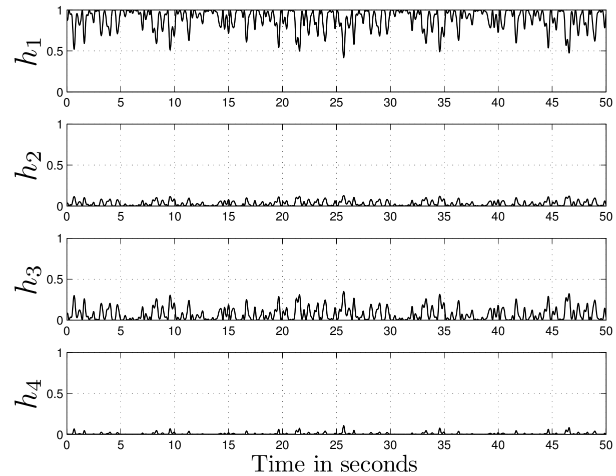

Fig. 6. Rule activation when the system is stabilized by a controller.

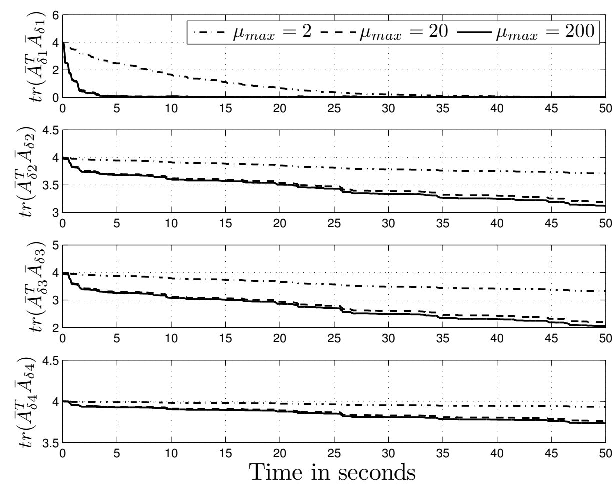

Fig. 7. Uncertainty estimation error comparison with and without the controller.

The uncertainty estimates obtained after 50 s are

$$\widehat{A}_{\delta 1} = \begin{bmatrix} -0.28 & 0.01 & 0 & 0 \\ 0.30 & -0.56 & 0.01 & 0 \end{bmatrix}$$
$$\widehat{A}_{\delta 2} = \begin{bmatrix} -0.01 & 0 & 0 & 0 \\ 0.01 & -0.05 & 0 & 0 \end{bmatrix}$$
$$\widehat{A}_{\delta 3} = \begin{bmatrix} -0.04 & 0 & 0 & 0 \\ 0.03 & -0.12 & 0 & 0 \end{bmatrix}$$
$$\widehat{A}_{\delta 4} = \begin{bmatrix} 0 & 0 & 0 & 0 \\ 0 & -0.01 & 0 & 0 \end{bmatrix}$$

The uncertainty estimation error obtained in closed loop is higher than then error obtained in open loop. It can be seen from Figure 7 that the estimation error converges faster in the case of rule R_1. This is due to the fact that the stabilizing action by the controller takes the states of the system towards zero. Since θ_2 is close to zero, the degree of activation of R_1 is high, but the activation of the other rules is lower.

VI. Conclusions and discussions

In this paper we presented an adaptive observer to estimate uncertainties in the model of a 2-DOF robot arm. The results show that the value of the upper bound on the uncertainty norm μ_{max} for which the adaptive observer is designed behaves as an uncertainty convergence rate. However, in our model, uncertainty is present only in the state matrices. This behavior has to be verified in situations where uncertainties exist in the input matrices as well. The uncertainty estimates were used to obtain an updated model. Simulation results indicate that with lower uncertainty in the updated model, the controller can guarantee stability with a higher decay rate.

It is important to note that in general the value of μ_{max} to be used will depend on the extent to which the initial uncertain model represents the plant, with larger mismatch between the plant and the model requiring higher values of μ_{max}.

The possibility to exploit the structure of the uncertainty in the TS model in designing the experiments was also discussed. However, since not all rules are activated with a high degree, in this case, the uncertainty convergence rate becomes very small for those rules that are not activated. Hence, the experiment duration and the type of input signal required to obtain better estimates for these other rules should be further investigated.

Acknowledgment

This work was supported by a grant of the Romanian National Authority for Scientific Research, CNCS – UEFISCDI, project number PN-II-RU-TE-2011-3-0043, contract number 74/2011.10.05.

References

[1] C. Fantuzzi and R. Rovatti, “On the approximation capabilities of the homogeneous Takagi-Sugeno model,” in *Proceedings of the Fifth IEEE International Conference on Fuzzy Systems*, New Orleans, Louisiana, September 1996, pp. 1067–1072.

[2] Zs. Lendek, T. M. Guerra, R. Babuška, and B. De Schutter, *Stability Analysis and Nonlinear Observer Design Using Takagi-Sugeno Fuzzy Models*, P. J. Kacprzyk, Ed. Springer, 2010.

[3] Zs. Lendek, J. Lauber, T.-M. Guerra, R. Babuška, and B. De Schutter, “Adaptive observers for TS fuzzy systems with unknown polynomial inputs,” *Fuzzy Sets and Systems*, vol. 161, no. 15, pp. 2043–2065, 2010.

[4] H. Ohtake, K. Tanaka, and H. Wang, “Fuzzy modeling via sector nonlinearity concept,” in *Proceedings of the Joint 9th IFSA World Congress and 20th NAFIPS International Conference*, vol. 1, Vancouver, Canada, July 2001, pp. 127–132.

[5] T. Takagi and M. Sugeno, “Fuzzy identification of systems and its applications to modeling and control,” *IEEE Transactions on Systems, Man, and Cybernetics.*, vol. 15, pp. 116–132, 1985.

[6] K. Tanaka and H. O. Wang, *Fuzzy Control Systems Design and Analysis - A Linear Matrix Inequality Approach*. John Wiley & Sons, Inc, 2001.